INTERNATIONAL JOURNAL OF HYDROGEN ENERGY 48 (2023) 37579–37593

Available online at www.sciencedirect.com

ScienceDirect

journal homepage: www.elsevier.com/locate/he

Feasibility analysis of green hydrogen production from wind

*Angelica Liponi, Andrea Baccioli, Lorenzo Ferrari**

Department of Energy, Systems, Territory and Construction Engineering, University of Pisa, Pisa, Italy

HIGHLIGHTS

- Effects of overall size and number of separated electrolysis groups are investigated.
- Stack degradation included in the electrolyzer model.
- Higher production in 2-group configurations compared to equivalent single-group ones.
- Minimum hydrogen selling price between 4.5 and 6.5 €/kg required for profitability.
- Dividing the electrolysis plant into more than 2 groups didn't result profitable.

ARTICLE INFO

Article history:
Received 23 January 2023
Received in revised form
8 April 2023
Accepted 4 May 2023
Available online 25 May 2023

Keywords:
Wind energy
Alkaline electrolysis
Degradation model
Techno-economic analysis
Hydrogen price

ABSTRACT

Renewable hydrogen production has an important role in global decarbonization. However, when coupled with intermittent and variable sources, such as wind or PV, electrolyzers are subjected to part-load and dynamic operation. This can lead to low utilization factors and faster degradation of the electrolyzers and affect the specific hydrogen cost. The design and sizing of such electrolysis systems are fundamental to minimize costs. In this study, several configurations of an electrolysis system producing green hydrogen from a 39 MW-wind farm are compared. The effects of both the size of the plant and the number of separated groups into which it is divided are investigated. Dividing the plant into two separated groups resulted to be enough to increase hydrogen production; a further increase in the number of groups didn't produce significant differences. The most profitable configurations resulted that with one or two groups, depending on the hydrogen selling price.

Introduction

Hydrogen is recognized to be one of the key elements that will help in the global decarbonization efforts [1]. In order to reduce carbon dioxide (CO_2) emissions, the deployment of renewable energies (RE), in particular wind and photovoltaic (PV), for electricity production is continuously increasing. The high share of these sources is causing an increasing need for energy storage systems and the transition to multi-vector energy systems. Hydrogen production through water electrolysis allows the conversion of electrical energy into chemical energy and can contribute to making RE penetration in the grid more reliable and reducing RE curtailment [2]. Furthermore, hydrogen allows the storage of significant amounts of energy even for extended periods [3].

Hydrogen is also required by many industrial processes, such as ammonia production, steel making and oil refining, where it is currently produced for the greatest part with fossil fuel-based methods. Its replacement with electrolytic

* *Corresponding author.*
E-mail addresses: angelica.liponi@destec.unipi.it (A. Liponi), andrea.baccioli@unipi.it (A. Baccioli), lorenzo.ferrari@unipi.it (L. Ferrari).
https://doi.org/10.1016/j.ijhydene.2023.05.054

hydrogen produced using RE will therefore give a great contribution to decarbonize these sectors [4], together with the adoption of carbon capture systems. Water electrolysis technologies can be divided into low-temperature (alkaline and polymer electrolyte membrane electrolyzers) and high-temperature electrolyzers (solid-oxide electrolyzers) [5]. Among these technologies, the alkaline one is the most mature and widespread [6]. However, alkaline electrolyzers have some limitations when operating with fluctuating REs. Indeed, they must operate in the range of 20–100% of the nominal power [7] for safety reasons since, at lower loads, the ratio of hydrogen to oxygen increases and there is the risk that it exceeds the explosion limit [8]. When coupled to fluctuating renewable sources, electrolyzers are subjected to dynamic and part-load operation and to frequent shutdowns that can cause faster stack degradation [9].

Many studies deal with coupling of water electrolysis with RE, in particular wind and solar PV, and with the sizing of these systems. The design and the choice of the sizes of electrolysis systems coupled to REs is a trade-off between the maximization of RE utilization and the minimization of hydrogen production costs. On one side, a higher nominal power of the electrolysis system increases the RE utilization. On the other side, it leads to a decrease in the electrolyzers' utilization factor and, consequently, to an increase in the specific hydrogen production cost, as highlighted also by Khan et al. [10]. The effects of the source variability related to the location and climate conditions on techno-economic performances have been investigated both for wind [11] and PV sources [12].

In order to mitigate production fluctuations due to RE power input variability, electrical storage can be added to the system. The choice of the storage size should be a compromise between the improvement in the operation of the electrolysis system and the limitation of costs. Liponi et al. [13] investigated the effects of the presence of a battery on the mitigation of fluctuations of hydrogen production by an electrolyzer from wind energy. The adopted management strategy assigned the electrolyzer power input as a function of both the battery state of charge and a moving average of the wind turbine power. Battery capacities of at least about 6 h were necessary to achieve significant effects but led to non-competitive hydrogen costs. Fang and Liang [14] adopted a modular adaptive control strategy to optimize the electrolyzer operation to overcome wide power fluctuations in a wind-hydrogen system. Supercapacitors were integrated to absorb instantaneous power fluctuations. They found a significant reduction in the number of electrolyzer start-stop switching and an increase in hydrogen production in comparison with other control strategies.

When an electrolysis system is coupled with variable and intermittent power input such as RE one, another option to limit frequent shutdowns and consequent fast degradation is to keep the electrolyzers in warm stand-by state for short periods. In this way, by consuming a small amount of electricity, the stack lifetime can be increased. Matute et al. [15] developed a multi-state techno-economic model for the optimal operation of a power-to-hydrogen system. By testing it with real data and comparing it with a model with only two states, they found the multi-state model more profitable. Zheng et al. [16] proposed an alkaline electrolyzer model taking into account temperature variations and electrolyzer state transitions and employed it in an optimal day-ahead operation problem of a wind-electrolyzer system. Varela et al. [17] proposed an optimal scheduling model for an alkaline electrolysis system for the efficient conversion of RE into hydrogen. Their model takes into account different operational states and transitions of the electrolyzers. They applied the model to a case study of a 50 MW wind plant. They found that the optimal number of electrolyzers corresponded to an overall nominal power equal to 54% of the wind power peak and was capable of using 89.7% of the annual available energy. They did not consider any grid electricity contribution and found 764 start-up/shutdown cycles evenly distributed among the units.

In the case of large-scale electrolysis plants, multi-stack systems are adopted. The optimal configurations and power allocation strategies of such systems are worthy of investigation in order to both maximize the overall efficiency and/or minimize stacks degradation. Lu et al. [18] proposed an optimization of a power allocation strategy for a wind-hydrogen system with a multi-stack PEM water electrolyzer by considering the degradation status of each stack. Five different operating conditions were considered to determine the stack degradation rate during operation: maintaining, low power fluctuation, constant turning power, high power fluctuation, and constant rated power. The proposed strategy was compared to other strategies (average allocation, daisy chain allocation, and optimal efficiency allocation) and showed an energy efficiency comparable to that of the optimal efficiency allocation strategy (the highest one). Meanwhile, the single-stack degradation was almost the same for each stack and it was lower than the stack degradation (averaged among the stack) obtained with the other power allocation strategies. Hong et al. [19] proposed a control strategy based on the segmented-fuzzy control for improving the overall efficiency of multi-electrolyzer systems for hydrogen production from wind. Luxa et al. [20] developed a multi-stack PEM modeling and simulation framework by using a multi-linear model class. The model included a linear stack degradation model and an electrolyzer controller for allocating the operating power to each stack. Rizwan et al. [21] proposed a shared balance of plant (BoP) and power supply design for an industrial-scale alkaline electrolyzer plant that reduces capital costs with minimum negative effects on operational flexibility and performance. The electrolyzer stacks were assumed at different stages of their lifetime and consequently had different performances because of stack degradation. They found that the layout with separate BoP and power systems has higher capital investments but offers greater operational flexibility when the electrolyzer stacks are degraded. Results showed that individual BoP per stack (with higher capital costs) is optimal when the plant is expected to operate at high capacity. For shared BoP, the hydrogen production was increased by 8–12% when operated with variable lye flowrate compared to fixed lye flowrate [21].

In this study, a techno-economic comparison of several configurations of an alkaline electrolysis system for green hydrogen production from a 39 MW grid-connected wind farm has been carried out. Hydrogen is produced with wind

electricity while grid electricity is used only to keep electrolyzers in stand-by for short periods of low wind power and, thus, limit the number of electrolyzers' shutdowns. The excess of wind electricity that is not used for the electrolysis process is sold to the grid. Each configuration has a different overall electrolysis capacity and consists of a different number of electrolysis groups that can operate separately. Each group consists of several 1 MW-electrolyzers that operate together at the same operating conditions and have shared power supply and BoP. The shared BoP allows a reduction of BoP capital costs because of the greater size of the components and consequently lower specific capital costs. The purpose is to investigate the effects of both the overall capacity of the electrolysis plant and the number of groups on the system operation and economic feasibility and to find the most profitable configuration.

Annual simulations of the system operation were performed for each configuration. An analysis of the operational states of the electrolysis groups and a comparison in terms of annual performance indicators have been carried out. The profitability of the configurations analyzed is evaluated by assuming several hydrogen selling prices with respect to the case without any electrolysis plant in which all wind electricity is sold to the grid.

System description and modeling

The system under investigation consists of an alkaline electrolysis system for green hydrogen production from a MW-scale grid-connected wind power plant. The electrolysis system is divided into several units (groups) of the same size that can operate separately. The effects of both the overall nominal power of the electrolysis system and the number of groups into which it is divided have been investigated. Several configurations of the electrolysis system characterized by different overall capacities up to a nominal power equal to the wind plant one and divided into a different number of groups have been compared through annual simulations of the system operation in MATLAB [22]. Power production data of an actual wind farm, located in South Australia, were taken as reference [23]. They consist in 5 min-averaged power data of one year (Fig. 1). The wind farm has a nominal power of 39 MW and consists of 13 turbines, each with a nominal power of 3 MW. Its capacity factor is 30.4%. The reason for choosing these data is to use power data that are representative of a real MW-scale wind farm. Indeed, actual power data already include turbine interaction effects on power production and power fluctuations that are typical of a wind farm and can not be easily taken into account by starting from wind speed data.

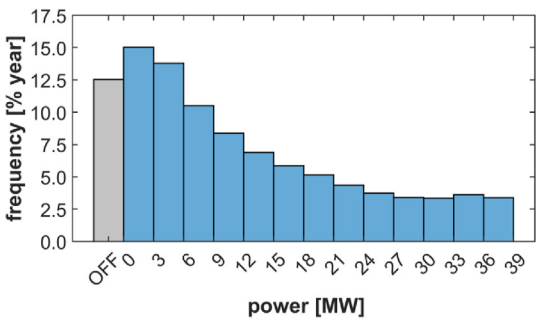

Fig. 1 – Annual distribution of the wind farm power output.

The wind power is sent to the electrolysis system as a priority while the possible exceeding power is released to the grid.

The electrolysis system is divided into several electrolysis groups that can operate separately. Each group consists of a number ($n_{elz\ per\ group}$) of 1 MW alkaline electrolyzers that operate simultaneously. Electrolyzers in the same groups have a shared balance of plant (BoP), including the separators, buffer tank, pump, and cooler in the lye circulation loop, and also power electronics and gas conditioning. This allows to reduce the number of BoP components and increase their size. In this way, their capital cost can be reduced. The same number of electrolyzers per group is assumed for each group of the same electrolysis system.

Several combinations of the number of electrolysis groups (n_{groups}), from 1 up to 39, and number of electrolyzers per group (from 1 up to 13) have been analyzed up to overall electrolysis capacities capable to use the whole nominal power of the wind plant (39 MW). Combinations with an overall electrolysis capacity under 7 MW were not considered since they could use just a very small fraction (less than 1/6) of the wind nominal power.

The power feeding the electrolysis system is equally divided among all the electrolysis groups in operation. Before being sent to the electrolyzer stacks, wind power is adjusted to the desired voltage by a transformer and converted to direct current by a rectifier. The power feeding the electrolyzers of the same group is equally divided among them. Consequently, electrolyzers of the same group operate all the time at the same conditions as one single bigger electrolysis unit and are subject to similar stack degradation throughout their lifespan.

The model of each single 1 MW electrolyzer takes into account both electrochemical and thermal aspects. The 3 MW alkaline electrolyzer adopted in Ref. [24] is taken as a reference. In addition, degradation effects on the polarization curve and consequent losses in the efficiency have been added to the model. An operating power range between 20% and 100% of the nominal power is imposed as a typical range for alkaline electrolyzers [7] to avoid safety problems at low current densities.

Given the electrical power input to each electrolyzer (P_{elz}), assigned at each time step by the management strategy, the power feeding the stack (P_{stack}) is determined by subtracting the power required by the BoP, which is assumed to be 8% of the power input. This percentage was derived from Ref. [24] at the nominal electrolyzer power. Then, the cell current (I_{cell}) and voltage (U_{cell}) are determined as a function of the stack temperature (T_{elz}) by solving the system of Eqs. (1) and (2) by means of the Newton iteration method.

$$P_{stack} = U_{cell} \cdot I_{cell} \cdot n_{cells} \tag{1}$$

$$U_{cell}(T_{elz}) = U_{rev}(T_{elz}) + (\alpha_1 + \alpha_2 \cdot T_{elz}) \cdot i + s \cdot \log\left[\left(\beta_1 + \frac{\beta_2}{T_{elz}} + \frac{\beta_3}{T_{elz}^2}\right) \cdot i + 1\right] \tag{2}$$

Eq. (1) states that the overall stack power is given by the product of the cell current (I_{cell}), cell voltage (U_{cell}), and the number of cells (n_{cells}) in the stack. Eq. (2) is the cell polarization curve in which the cell voltage is expressed as the sum of the reversible voltage, ohmic overpotential, and activation overpotential. The polarization curve is a function of the operating conditions and, in particular, of the temperature. Some of the coefficients in Eq. (2) are expressed as a function of the stack degradation level as described later.

The stack temperature (T_{elz}) is calculated through the thermal model proposed by Ulleberg [25], in which a lumped-capacitance model is applied and it is determined at each time step k as:

$$T_{elz}(k) = T_{elz}(k-1) + \frac{\Delta t}{C_{th}}\left[Q_{gen}(k-1) - Q_{loss}(k-1) - Q_{cool}(k-1)\right] \tag{3}$$

where $\Delta t = 300$ s is the time step of the simulations, C_{th} is the overall thermal capacitance, and Q_{gen}, Q_{loss}, and Q_{cool} are the internal heat generation, the total heat loss to the ambient, and the cooling heat, respectively.

The internal heat generation is calculated as:

$$Q_{gen}(k) = (U - U_{tn}) \cdot I \cdot n_{cells} \tag{4}$$

where U_{tn} is the thermo-neutral voltage.

The total heat loss is determined by assuming an overall thermal resistance (R_{th}) and a constant ambient temperature (T_a) of 25 °C as:

$$Q_{loss}(k) = (T_{elz}(k) - T_a) \,/\, R_{th} \tag{5}$$

In order to keep the stack temperature within the desired operating range, a cooling system is required to absorb the excess of heat produced. The cooling system consists of a cooling water heat exchanger with a simple on/off regulation. The cooling system is turned on when the stack temperature exceeds the upper threshold value of 73 °C and turned off when it drops below the lower threshold value of 67 °C. The cooling heat, Q_{cool}, is calculated as:

$$Q_{cool}(k) = \begin{cases} C_{cw}\,(T_{cwo}(k) - T_{cwi}) & \text{when the cooling system is on} \\ 0 & \text{when the cooling system is off} \end{cases} \tag{6}$$

where C_{cw} is the cooling water thermal capacitance, expressed in [J/K], and $T_{cwi} = 15$ °C and T_{cwo} are the cooling water inlet and outlet temperatures, respectively. The outlet cooling water temperature is calculated as:

$$T_{cwo}(k) = T_{cwi} + (T_{elz}(t) - T_{cwi}) \cdot \left[1 - \exp\left(-\frac{UA_{hx}}{C_{cw}}\right)\right] \tag{7}$$

where UA_{hx} is the product of the global heat transfer coefficient and the heat transfer area of the cooling water heat exchanger.

The values of the parameters for the thermal model (Table 1) are based on the reference model and appropriately scaled to be applied to the nominal power of the single electrolyzer that is 1/3 of that of the reference electrolyzer. Indeed, as for the thermal model, it should be considered that the thermal capacitance and resistance changes with the size. The UA_{hx} coefficient of the heat exchanger is chosen in order to have a proper temperature rise of the cooling water at nominal conditions of about 10 °C. The values adopted for the thermal model in this study are consistent with the corresponding values of electrolyzers with similar sizes having the same orders of magnitudes and can be considered reasonable for the aim of this study.

Table 1 – Parameters of the electrolyzer model.

Parameter	Value
n_{cells}	109
A_{cell}	1.3295 m^2
pressure	16 bar
$\%_{wt}$ KOH	25%
$\alpha_{1,0}$	$8 \cdot 10^{-5}$ Ω m^2
α_2	$-7.63 \cdot 10^{-7}$ Ω m^2/C
s_0	0.1795 V
β_1	$2 \cdot 10^{-3}$ m^2/A
β_2	$1 \cdot 10^{-5}$ m^2 K/A
β_3	35 m^2 K^2/A
η_F	0.86
C_{th}	$21.7 \cdot 10^6$ J/K
R_{th}	$3 \cdot 10^{-2}$ K/W
C_{cw}	$2.5 \cdot 10^4$ J/K
UA_{hx}	$5 \cdot 10^3$ W/K

As degradation occurs, the cell voltage-current relationship changes. In particular, at the same current density, overvoltage increases and, as a consequence, the electrolyzer efficiency decreases. There are no generic phenomenological degradation models for alkaline electrolyzers published, that can represent the influence on partial or dynamic load, as well as the number of on/offs. However, for the aim of this study, it is not essential to apply a degradation model that describes the electrochemical processes in detail. The effect of stack degradation has been included in the model by expressing the polarization curve also as a function of the stack degradation level. A constant degradation rate of 1 μV per equivalent operating hour at nominal load was assumed as typical value for alkaline electrolyzers. The maximum number of equivalent operating hours after which a stack replacement is needed ($h_{eq,max}$) is fixed equal to 100,000 h (projected 2030–2050 lifetime of alkaline electrolyzers [1]). As a consequence, the maximum degradation leads to a degradation overvoltage ($\Delta V_{nom,max\ degr}$) of 0.1 V (= 1 μV/h_{eq} · 100,000 h_{eq}) at the nominal current density.

At each time step, the degradation level is defined as the ratio between the equivalent operating hours ($h_{eq,degr}$) at that time step and the maximum equivalent operating hours:

$$L_{degr}(k) = h_{eq,degr}(k) / h_{eq,max} \tag{8}$$

The additional overvoltage ($\Delta V_{nom,degr}$) due to degradation at nominal power is assumed to be proportional to the degradation level and calculated at each time step as:

$$\Delta V_{nom,degr}(k) = L_{degr}(k) \cdot \Delta V_{nom,max\ degr} \tag{9}$$

The additional overvoltage changes with the current density. To take into account this, the polarization curve has been expressed as a function of the degradation level. In particular, the parameters s and α_1 are expressed as:

$$s = s_0 \cdot k_{degr}, \alpha_1 = \alpha_{1,0} \cdot k_{degr} \tag{10}$$

where k_{degr} is determined, by imposing the degradation overvoltage ($\Delta V_{nom,degr}$) at nominal current, as:

$$k_{degr}\left(L_{degr}\right) = \frac{V_{nom,degr}\left(L_{degr}\right) - U_{rev} \cdot \left(\alpha_2 \cdot T_{elz}\right) \cdot \frac{I_{cell,max}}{A_{cell}}}{\alpha_{1,0} \cdot \frac{I_{cell,max}}{A_{cell}} + s_0 \cdot \log\left(\beta \cdot \frac{I_{cell,max}}{A_{cell}} + 1\right)} \tag{11}$$

where $\beta = \beta_1 + \beta_2/T_{elz} + \beta_3/T_{el}T_{elz}$.

The equivalent operating hours of each electrolyzer used for determinate the degradation level ($h_{eq,degr}$) at each time step k are calculated as:

$$h_{eq,degr}(k) = \frac{\sum_{j=1}^{k} P_{elz}(j)}{P_{elz,nom}} \cdot \frac{\Delta t}{3,600\ s/h} + n_{OFF \to ON}(k) \tag{12}$$

where $n_{OFF \to ON}(k)$ is the number of electrolyzer start-ups from the OFF state from the beginning of the plant lifetime up to the time step k. Each transition from OFF to ON state is assumed equivalent to one operating hour.

The imposed minimum stack input power slightly increases with the degradation level to comply with the minimum allowed current density. Instead, the imposed maximum power input to the electrolyzer stack does not change with degradation and is set equal to the nominal stack power.

The hydrogen production rate, expressed in mols per second, and the electrolysis efficiency based on the lower heating value (LHV = 241 kJ/mol) are calculated at each time step as, respectively:

$$\dot{n}_{H_2} = \eta_F \frac{n_c \cdot I}{2 \cdot F} \tag{13}$$

$$\eta_{LHV} = \frac{\dot{n}_{H_2} \cdot LHV}{P_{elz}} \tag{14}$$

where η_F is the Faraday efficiency assumed to be 0.86, as reported in Ref. [24].

The annual hydrogen production ($M_{H_2,ann}$), expressed in kilograms, is calculated as:

$$M_{H_2,ann} = \frac{2.016}{1000} \cdot \sum_{k=1}^{105120} \dot{n}_{H_2}(k) \cdot \Delta t \tag{15}$$

The annual equivalent operating hours of each electrolyzer ($h_{eq,degr,ann}$) are calculated as:

$$h_{eq,degr,ann} = \frac{\sum_{k=1}^{105120} P_{elz}(k)}{105120 \cdot P_{elz,nom}} \cdot 8760 \frac{h}{y} + n_{OFF \to ON} \tag{16}$$

The annual utilization factor (UF) of each electrolyzer is defined as the ratio between average input power, including OFF periods, and the nominal electrolyzer power:

$$UF\ [\%] = \frac{\sum_{k=1}^{105120} P_{elz}(k)}{105120 \cdot P_{elz,nom}} \cdot 100 \tag{17}$$

The stack of each electrolyzer is supposed to be replaced when the degradation level reaches 100% or after a maximum of 10 years of operation. Consequently, the electrolyzer stack lifetime (Lt_{elz}), expressed in years, is determined as:

$$Lt_{elz} = \min\left(\frac{h_{eq,max}}{h_{eq,degr,ann}}, 10\right) \tag{18}$$

Therefore, the number of stack replacements (n_{repl}) required during the entire plant lifetime is determined as the maximum between the ratio between the plant lifetime (Lt_{pl}) and the stack lifetime, rounded down to the nearest whole number:

$$n_{repl} = \max\left(\left\lfloor \frac{Lt_{pl} - 0.01}{Lt_{elz}} \right\rfloor\right) \tag{19}$$

In Eq. (19), 0.01 is subtracted to the plant lifetime just to avoid counting a replacement that may occur just at the end of the plant lifetime. It is simply a mathematical expedient that do not alter the results.

Management strategy

A management strategy is applied in order to decide the operational state of each electrolysis group and the electricity flows. Wind power is supposed to feed the electrolysis system as a priority, i.e., whenever possible by respecting the imposed constraints. The excess power that can not be used by the electrolysis system is released to the external grid. Three operational states are defined for the electrolysis groups: ON, stand-by (SB), and OFF states. If the state of a group is ON, the electrolyzers of the group are operating at the same power that must be within the allowed operating power range. If the state of a group is OFF, all the electrolyzers of the group are OFF, no power is consumed, and no hydrogen is produced by the group. If the state of a group is SB, all the electrolyzers of the groups are kept in temperature and pressure, and no hydrogen is produced. The power consumption during SB is assumed to be 5% of the nominal power and to be provided by the grid. No power is provided by the grid for the electrolysis operation apart from that required for SB states.

The following further constraints are imposed:

- An electrolysis group can be turned ON from the OFF state only after a minimum time of 2 h.
- If the wind power is not sufficient to keep in the ON state all the groups operating in the previous time step, the maximum possible number of groups already operating are kept on, while the rest is put in SB state. First, the groups with a higher number of equivalent operating hours are switched SB.
- If the wind power exceeds the maximum allowed power of the groups operating in the previous time step, further groups are turned ON, if possible. The number of groups turned ON is the minimum number that allows to use the exceeding power as much as possible. First, the groups in SB for more time are turned ON. Then, if there are no more groups in SB, the groups that were OFF in the previous time step are turned on if possible and if the minimum imposed off time has been already reached. When switching groups from OFF to ON, the priority is given to the groups with a higher number of equivalent operating hours.
- If the electrolyzers of a group are not turned ON after a maximum duration of continuous SB state of half an hour, they are turned OFF.

The strategy adopted aims to limit as much as possible state changes. Furthermore, it aims to keep the equivalent operating hours of the groups as much similar as possible. The minimum OFF duration is imposed to avoid too frequent electrolyzers on/offs.

Analysis of the operational states of the electrolysis groups

In general, at the same overall electrolysis capacity, several configurations with a different number of electrolysis groups are possible. The lower is the number of groups, the greater is the number of 1 MW-electrolyzers per group. For example, for an overall electrolysis capacity of 24 MW, there are eight possible configurations ($n_{groups} \times n_{elzs\ per\ group}$): 1 × 24, 2 × 12, 3 × 8, 4 × 6, 6 × 4, 8 × 3, 12 × 2, and 24 × 1. Given an overall electrolysis capacity, the plant operation is influenced by the configuration adopted. Indeed, smaller and more numerous groups allow the system to operate even at lower wind power. On the other side, smaller groups have a narrower power operating range and, therefore, they may be more frequently subject to changes in the operational state. As an example, Fig. 2 shows the operation of all the groups in three different configurations with the same overall nominal electrolysis power of 24 MW during a 7-day period. The first configuration has six electrolysis groups, each with four 1 MW-electrolyzers; the second one has two electrolysis groups, each with twelve 1 MW-electrolyzers; and the third one has only one electrolysis group made of twenty-four 1 MW-electrolyzers operating always together.

By increasing the number of groups of a smaller size, changes in the operational state are more frequent. On the other side, the electrolysis system is in operation (with at least one group) for a greater percentage of time. It can be notice that there are short frequent SB periods between two successive ON states when wind power has strong fluctuations. This is more marked in the configurations with more and smaller groups. SB state allows to avoid too frequent shutdowns and consequent losses in production.

For each configuration, each electrolysis group operates separately and, consequently, has its own power input and production trend over time. However, because of the adopted management strategy, all the groups of the same configuration have similar annual operating conditions. This was confirmed by the results obtained. For this reason and for making an easier comparison, the results obtained for each configuration that are shown in the following are averaged among all the groups of each configuration.

At the same overall nominal electrolysis power, by increasing the size of each group (i.e., by reducing the number of groups), the average annual percentage of time during which a group is in operation (ON state) increases (Fig. 3). In the configurations with only one group, the operating power range of the single larger group is wider than in the configurations with a higher number of smaller groups. Therefore,

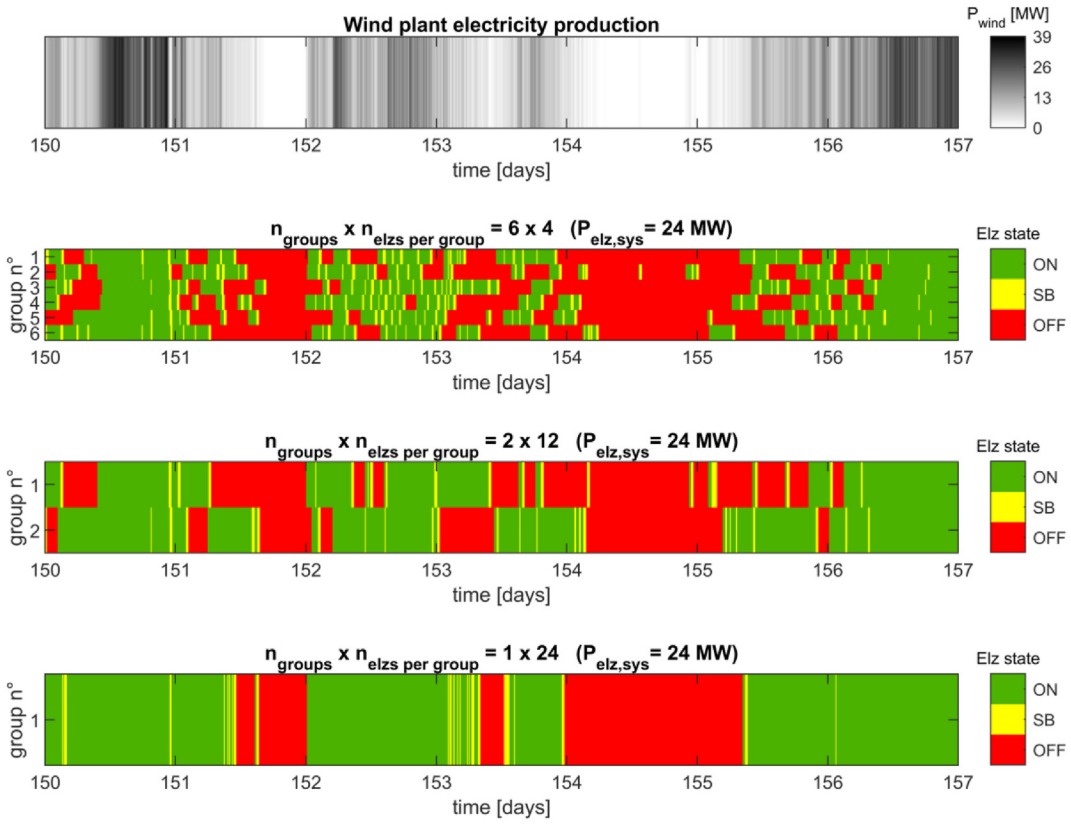

Fig. 2 – Example of operational states of the electrolysis groups for a 7-day period in three cases with a different number of groups (6, 2, and 1 groups) at the same overall electrolysis capacity of 24 MW.

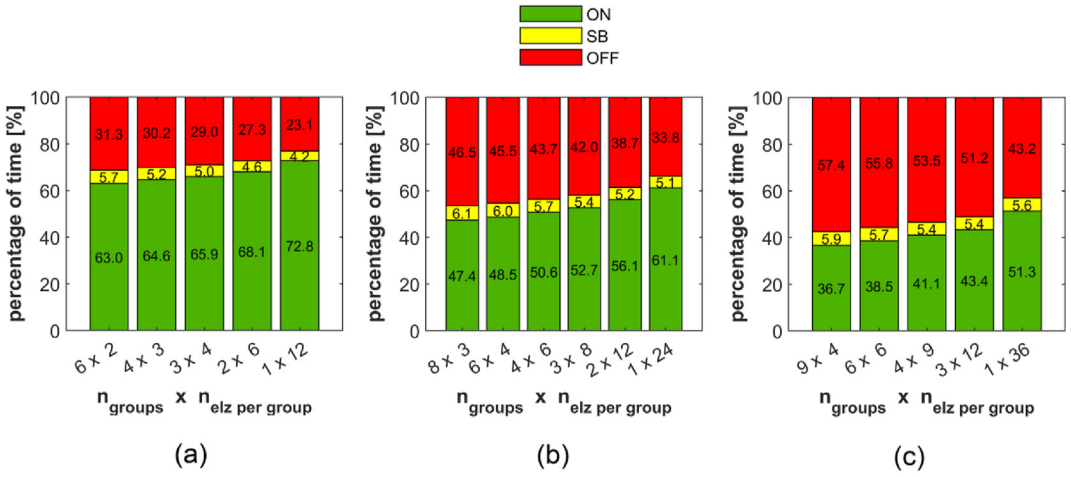

Fig. 3 – Annual percentage of time during which each electrolysis group is in the ON, SB, and OFF states (averaged among all the groups for each configuration) for configurations with a different number of electrolysis groups at the same overall nominal electrolysis power of (a) 12 MW, (b) 24 MW, and (c) 36 MW.

the single group can be in operation for more time. It must be pointed out that this does not mean that the overall plant produces more hydrogen or is in operation for more time in the configuration with only one group. Indeed, in the case of two or more groups, each group can operate in a different period and globally cover a greater percentage of the year in comparison to the configuration with one group. In confirmation of this, as shown later (Fig. 7b), the utilization factor of the electrolyzers is about the same or even slightly higher in the configurations with more than one group.

The overall SB duration, averaged among all the groups of each configuration, accounts for between about 4 and 6% of the year in all the configurations analyzed. It decreases with the decrease in the number of groups when the overall nominal power is under 25 MW (Fig. 3a–b). This is consistent with the more frequent changes in the operational states in the configurations with more electrolysis groups. For overall electrolysis power greater than 25 MW, differences in the overall group-averaged SB duration decrease (as occurs in Fig. 3c).

The distributions of SB durations (Fig. 4) give information on how much the SB state helps in limiting the number of shutdowns and on the appropriateness of the maximum duration imposed. A maximum SB duration of 30 min was imposed by the management strategy, after which, if the group was not turned on, it was turned off. In all the configurations, the two more frequent SB durations are the smallest and the greatest one. Slightly more than 1/3 of the SB periods lasts the maximum time of 30 min for all the configurations. This high frequency is due to imposed maximum SB duration: an electrolyzer that would have been in the SB state for more than 30 min is forced to be turned off. Instead, the frequency of the shortest (5 min-) SB periods is more variable depending on the configuration. Generally, SBs that last only 5 min are less frequent (in percentage terms) in the configurations with a higher number of groups. The rest of SB durations (10–25 min) accounts for between about 25 and 35% of the total number of SBs.

The distribution of OFF durations has a decreasing trend with the OFF duration as can be seen from the decreasing

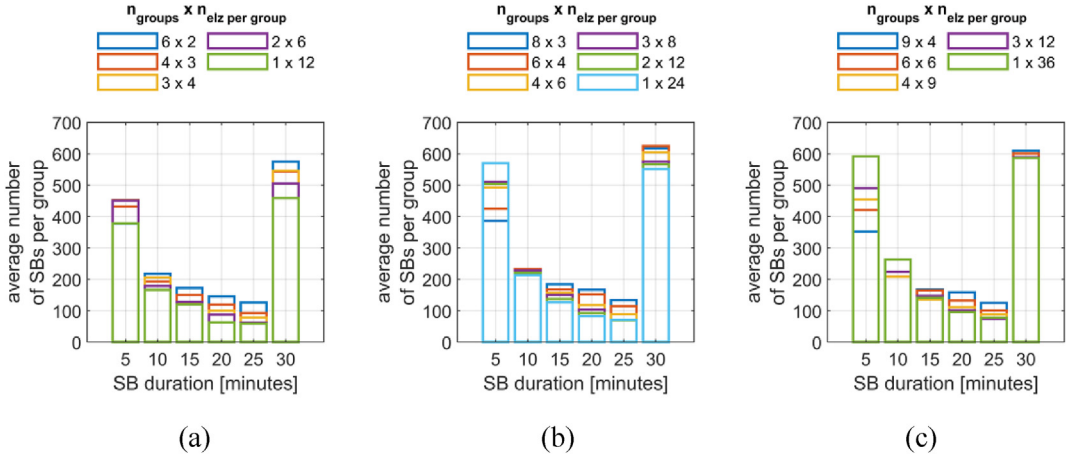

Fig. 4 – Group-averaged annual distribution of SB duration for several configurations with a different number of electrolysis groups at the same overall nominal electrolysis power of (a) 12 MW, (b) 24 MW, and (c) 36 MW.

slope of the cumulative frequency in Fig. 5. The ordinate of the points on the curves of the graphs (Fig. 5) represents the group-averaged annual number of OFF periods that last less than the OFF duration indicated by the abscissa. The abscissa of the point marked by the "x" symbol is the maximum OFF duration occurred (the averaged value among all the groups) while the y-coordinate is the annual (group-averaged) number of OFF periods. The most frequent OFF lengths are the shortest ones, as can be observed from the steeper slope at low average OFF durations. Reducing the number of short OFF periods, which can be seen as an index of the frequency of shutdowns, has a positive effect on the electrolyzers lifetime. The percentage of short OFF periods with a length under 2.5 h depends on the configuration and varies between 14 and 57%. It decreases with the increase in the overall nominal power and with the increase in the number of groups. The annual maximum OFF duration can reach about 4–5 days (as indicated by the marker "x" in Fig. 5). Most of the OFF periods (>50%) have a duration of less than 6 h (as can be seen from the marker "+", indicating the cumulative frequency of the 50% of the annual OFF events). According to these results, by allowing grid electricity support for a maximum of 6 continuous hours when wind power is not enough to continue to operate an electrolysis group, the number of OFF periods would be at least halved.

Most of the annual overall OFF duration (>50%) is constituted by less than one-fourth of the total number of OFF periods with the highest OFF durations as can be observed by the increased slope of the curves between the 50%- and the 100%-annual cumulative OFF duration (marked by the symbols "+", and "x", respectively, in Fig. 6). This is more accentuated in the configurations with only one electrolysis group. To eliminate this part of the cumulative OFF duration, consisting of the longest OFF periods, would require a large amount of external

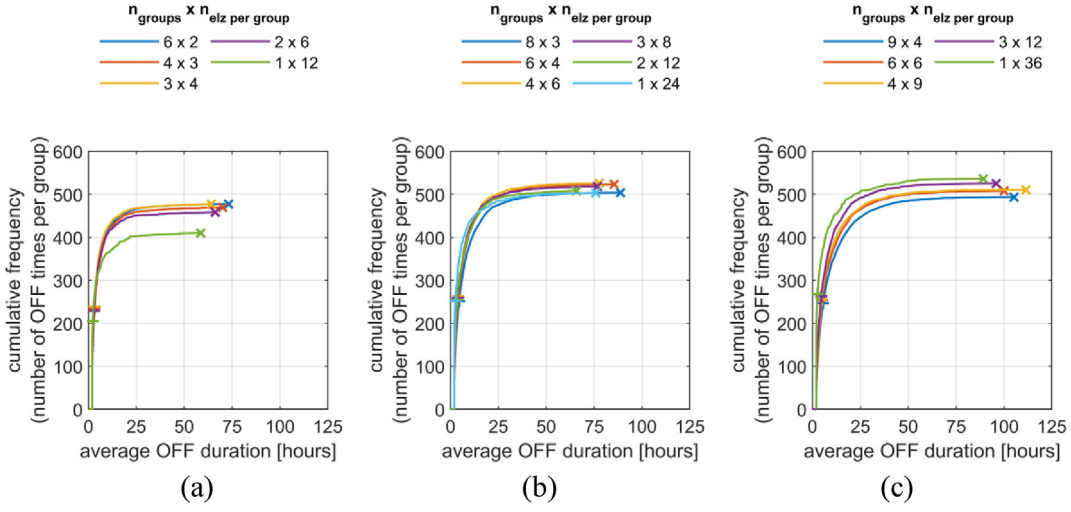

Fig. 5 – Group-averaged cumulative frequency of OFF durations for several configurations with a different number of electrolysis groups at the same overall nominal electrolysis power of (a) 12 MW, (b) 24 MW, and (c) 36 MW "+" indicates 50% of the annual OFF events. "x" indicates 100% of the annual OFF periods.

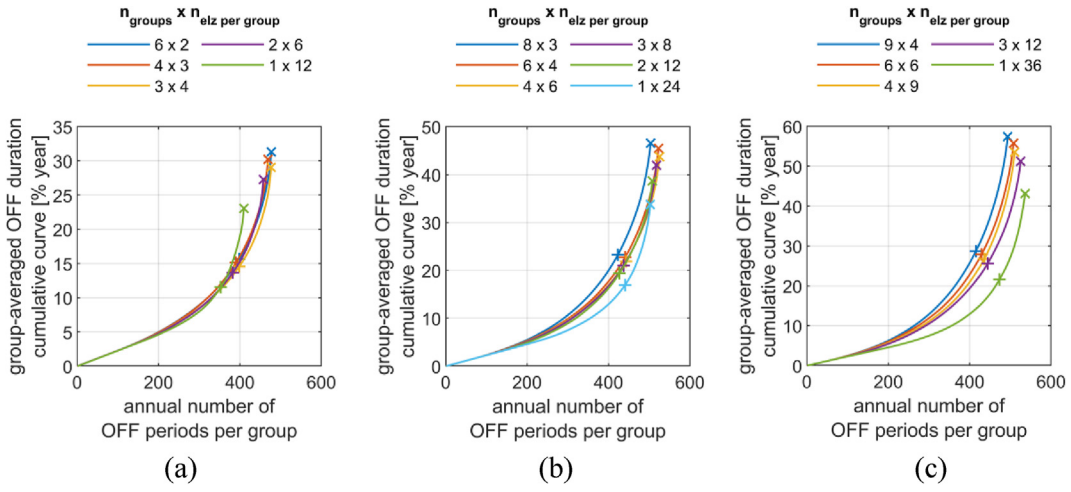

Fig. 6 – Group-averaged OFF-duration cumulative sum in ascending order for several configurations with a different number of electrolysis groups at the same overall nominal electrolysis power of (a) 12 MW, (b) 24 MW, and (c) 36 MW "+" indicates 50% of the annual cumulative OFF duration. "x" indicates the annual cumulative OFF duration.

electricity or large electric storage and would not be environmentally (in the case of non-RE electricity support) nor economically convenient. Furthermore, the presence of long OFF periods affects to a lesser extent the annual number of electrolyzer shutdowns in comparison with the more frequent shorter OFF periods.

Annual performance indicators

All the configurations analyzed are compared in terms of several annual performance indicators. The first indicator is the annual overall hydrogen production (Fig. 7a). Annual hydrogen production generally increases with the overall electrolysis capacity since more wind electricity can be converted into hydrogen at higher electrolysis capacities. In the configurations with only one group, the increase in hydrogen production with the increase in the overall nominal electrolysis power is lower, especially when the electrolysis power is above about half the wind nominal power. This is accentuated for increasing overall electrolysis capacities.

Given the same number of groups, when the electrolysis capacity increases, the minimum operating power of the system increases in all the configurations since the size of each group increases. However, in the case with only one group, the minimum operating power increases more. This causes the impossibility of using wind power lower than that minimum value and, consequently, a lower hydrogen production. Even if the percentage of the annual time during which each electrolysis group is in operation is higher in the case with only one group (Fig. 3), the annual time during which at least one group of the plant is in operation is lower in comparison to the configurations with more than one group. The presence of two groups is already enough to avoid a marked reduction of the overall hydrogen production at the greatest overall electrolysis capacities.

Furthermore, a small reduction in the annual overall hydrogen production with the increase in the overall electrolysis capacity is obtained at the highest overall nominal power in the configurations with only one group.

In general, when increasing the overall electrolysis capacity, the increase in the hydrogen production (Fig. 7a) is obtained at the expense of a reduction in the utilization factor of the electrolyzers (Fig. 7b) and an increase in the number of operational state changes. In turn, this has a negative impact on the specific hydrogen production costs.

At the same number of electrolysis groups, the number of start-ups increases up to a certain overall electrolysis capacity and then decreases for higher capacities (Fig. 8). The overall electrolysis capacity at which the maximum number of start-ups is reached depends on the number of groups and is generally greater in the case with fewer groups. At low overall electrolysis capacities, the configurations with fewer electrolysis groups show a lower number of start-ups. The opposite happens at higher capacities (greater than about 25 MW).

The annual number of start-ups from the OFF state, together with the utilization factor of the electrolyzers, influences stack degradation. In turn, stack degradation decreases the electrolyzers' efficiency and, consequently, the hydrogen production. Furthermore, it may cause the need of an early stack replacement. Stack degradation decreases with the increase in the overall nominal electrolysis power (Fig. 9) because of the decrease in the utilization factor of the electrolyzers (Fig. 7b). At greater overall nominal electrolysis power, stack degradation is lower in the configurations with only one group compared to the other configurations at the

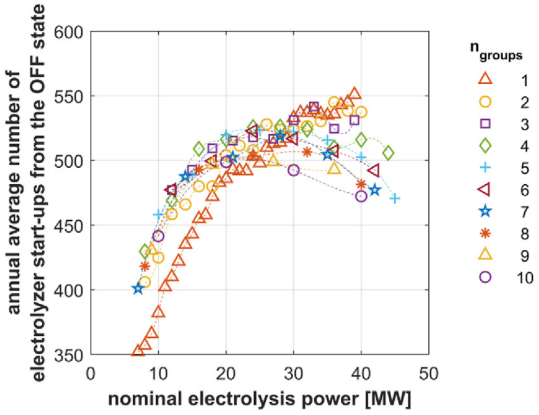

Fig. 8 – Annual average number of start-ups from the OFF state of each electrolyzer *vs* overall nominal electrolysis power for a different number of electrolysis groups.

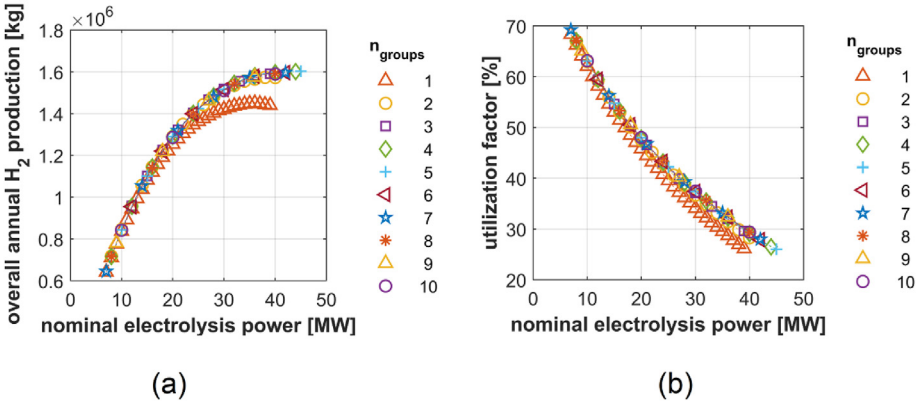

Fig. 7 – (a) Annual overall hydrogen production and (b) group-averaged utilization factor of the electrolyzers *vs* overall nominal electrolysis power for a different number of electrolysis groups.

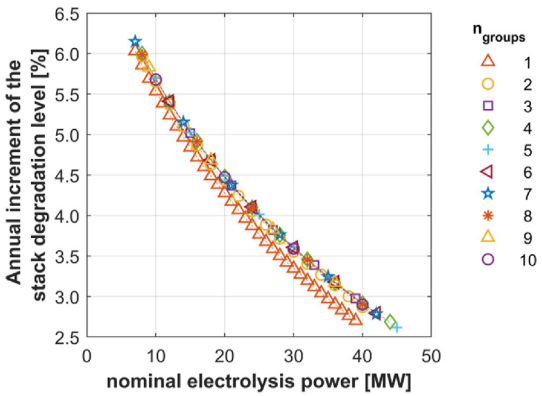

Fig. 9 – Annual increment of the stack degradation level *vs* overall nominal electrolysis power for a different number of electrolysis groups.

same overall electrolysis capacity. Instead, there are no relevant differences in the annual stack degradation among the configurations with more than one group. This result is consistent with the lower utilization factor of the electrolyzers in the case with only one group that is enough to compensate the missed reduction of start-ups at the highest overall electrolysis capacities (Fig. 8). The annual average stack degradation level varies between 2.5 and 6.5%, depending on the configuration. As a consequence, stacks are always replaced after the maximum imposed period of 10 years, and at that moment, the maximum degradation is not yet reached.

Economic and feasibility analysis

In order to compare all the different sizes and configurations of the electrolysis system in economic terms, the levelized cost of hydrogen and the equivalent hydrogen price (EHP), defined below, are determined.

The levelized cost of hydrogen (LCOH) is calculated as the sum of the contribution given by the capital and operation and maintenance costs of the electrolysis plant, including stack replacements ($LCOH_{elz\ sys}$); the contribution of the wind electricity cost ($LCOH_{w\ el}$); and the contribution of the grid electricity cost purchased for keeping the electrolyzers in the SB state ($LCOH_{SB\ el}$). The first contribution is given by the ratio between the annualized cost of the electrolysis system ($C_{elz,ann}$) and the annual hydrogen production ($M_{H_2,ann}$).

$$LCOH_{elz\ sys} = C_{elz,ann} / M_{H_2,ann} \tag{20}$$

The annualized cost of the electrolysis system, including operation and maintenance costs and the possible stack replacement cost, is determined as:

$$C_{elz,ann} = \mathrm{CRF} \cdot \left[C_{cap} + C_{repl}\right] + C_{O\&M} \tag{21}$$

where C_{cap} is the capital cost of the electrolysis system, C_{repl} is the cost of stack replacement, and $C_{O\&M}$ is the annual operation and maintenance cost, assumed to be 2% of the capital cost [26].

The capital recovery factor, CRF, is given by:

$$\mathrm{CRF} = \mathrm{IR} \cdot (1+\mathrm{IR})^{Lt_{pl}} \Big/ \left[(1+\mathrm{IR})^{Lt_{pl}} - 1\right] \tag{22}$$

in which an interest rate (IR) of 5% [27] is assumed.

The specific capital cost of a single electrolyzer ($c_{elz,ref}$), including BoP, is assumed to be 1100 €/kW [28]. Half of this cost is assumed to be the cost of BoP (including power electronics and gas conditioning) [28]. When the electrolysis groups have more than one electrolyzer, the BoP is shared by all the electrolyzers of the group. The specific cost of the electrolyzers without including the shared BoP is supposed to remain the same in all the cases. Instead, the specific cost of BoP is supposed to decrease with the increase in the size of each group. A specific cost ($c_{BoP,ref}$) of 550 €/kW is assumed for the reference size of 1 MW (the size of the single electrolyzer) that lead to a reference BoP capital cost ($C_{cap,BoP,ref}$) of $5.50 \cdot 10^5$ €. The generally adopted exponential law was used to evaluate the BoP cost at different sizes of the groups. The BoP cost is calculated for each group as:

$$C_{\mathrm{cap,BoP},group} = C_{cap,BoP,ref} \cdot \left(\frac{n_{elz\ per\ group}}{1}\right)^{f_{scale}} \tag{23}$$

A scale factor, f_{scale}, of 0.677 was assumed as in Ref. [28].

The capital cost of each group is determined as the sum of the cost of the stacks and the cost of the BoP. The capital cost of the overall electrolysis system (C_{cap}) is the sum of the capital costs of the electrolysis groups.

Since all the groups are operated to have a similar degradation level, all the stacks are supposed to be replaced in the same period. Therefore, the cost of stack replacements is determined as:

$$C_{repl} = \begin{cases} n_{groups} \cdot n_{elz per\ group} \cdot \sum_{r=1}^{n_{repl}} 0.3 \cdot c_{elz,ref} \cdot P_{elz,nom}\ (1+\mathrm{IR})^{-r\ \cdot\ Lt_{elz}} & \text{if } n_{repl} > 0 \\ 0 & \text{if } n_{repl} = 0 \end{cases} \tag{24}$$

In Eq. (24), the replacement cost of each stack is assumed to be 30% of the overall capital cost [29] of a single electrolyzer.

The annual overall operation & maintenance cost of the electrolysis system, $C_{O\&M}$, is assumed to be 2% of the capital cost [26].

The contribution of wind electricity cost to the LCOH is given by:

$$LCOH_{w\ el} = \frac{E_{w \rightarrow elz\ sys,ann} \cdot c_{w\ el}}{M_{H_2,ann}} \tag{25}$$

The contribution of grid electricity cost for SBs to the LCOH is given by:

$$LCOH_{SB\ el} = \frac{E_{grid\rightarrow elz\ sys\ (SB),ann} \cdot c_{SB\ el}}{M_{H_2,ann}} \quad (26)$$

An average specific cost of wind electricity of 40 €/MWh$_{el}$ is assumed by considering the projected decrease of wind levelized cost of electricity and the 2019 global weighted-average levelized cost of electricity for onshore wind of 53 $/MWh, reported by IRENA [30]. A slightly higher average electricity cost of 60 €/MWh$_{el}$ is assumed for grid electricity used during SB states.

The second economic parameter defined and evaluated to make a comparison of the configurations of the electrolysis plant is the equivalent hydrogen price (EHP). It has been defined as the price at which the hydrogen produced should be sold to have the same net income that would be obtained by selling all the wind electricity directly to the grid. Accordingly, it was calculated as:

$$EHP = \frac{E_w \cdot p_{sell,w\ el} + C_{elz,ann} + E_{grid\rightarrow elz\ sys\ (SB),ann} \cdot c_{SB\ el} - p_{sell,w\ el} \cdot (E_{w\rightarrow grid,ann})}{M_{H_2,ann}} \quad (27)$$

In Eq. (27), the first addend in the numerator represents the annual income in the case without electrolytic hydrogen production, in which all the wind electricity produced (E_w) is sold at the price $p_{sell,w\ el}$. The second addend is the annualized cost of the electrolysis system. The third addend is the annual cost for purchasing grid electricity for SBs at the price $c_{SB\ el}$. Finally, the subtrahend is the annual revenue from selling the remaining wind electricity to the grid ($E_{w\rightarrow grid,ann}$) at the same selling price of the case without hydrogen production ($p_{sell,w\ el}$). For this evaluation, a fixed selling price of wind electricity to the grid of 50 €/MWh and a slightly greater purchase price of grid electricity for SBs of 60 €/MWh were imposed.

Finally, for all the configurations analyzed, the difference in the annual gain (ΔG) between the cases with and without the electrolysis system has been evaluated by assuming a hydrogen selling price. Three values of hydrogen selling price ($p_{H_2,sell}$) have been considered: 5, 7.5, and 10 €/kg.

$$\Delta G = p_{H_2,sell} \cdot M_{H_2,ann} + p_{sell,w\ el} \cdot (E_{w,ann} - E_{w\rightarrow elz\ sys,ann}) - c_{SB\ el} \cdot E_{grid\rightarrow elz\ sys\ (SB),ann} - C_{elz\ sys,ann} - p_{sell,w\ el} \cdot E_{w,ann} \quad (28)$$

Following this definition, when the hydrogen selling price is greater than EHP, ΔG is positive and, therefore, it is profitable to add the electrolysis plant to the wind farm.

The levelized cost of hydrogen (Fig. 10) increases with the overall electrolysis capacity and varies between 3.9 and 5.9 €/kg, depending on the configuration. Indeed, only wind electricity is used for hydrogen production. This causes a decrease in the utilization factor of the electrolyzers (and, consequently, in the hydrogen production of each electrolyzer) when the overall electrolysis capacity increases while the capital cost increases. At the same electrolysis capacity, the LCOH of the configuration with only one group is the lowest for nominal capacities of up to about 28 MW. At higher electrolysis capacities, it becomes more convenient to have two groups. At low capacities, the configurations with only one group have a lower capital cost of BoP due to the greater BoP size in comparison to configurations with more groups and, at the same time, hydrogen production is almost the same. At higher capacities, even if they have lower capital costs of BoP, their hydrogen production is lower than that of the configurations with at least two groups. This is the reason why the lowest LCOH is obtained with configurations with two groups. It results not convenient to have more than two groups for any of the considered overall electrolysis capacities.

The equivalent hydrogen price (EHP), defined by Eq. (27), increases with the overall electrolysis capacity (Fig. 11) and varies between 4.5 and 6.5 €/kg, depending on the configuration. The reason is that at low electrolysis capacities, the utilization factor is higher. This lowers the specific costs related to the electrolysis plant. As a consequence, lower hydrogen selling prices are required to obtain the same net income as that in the case of directly selling all the wind electricity to the

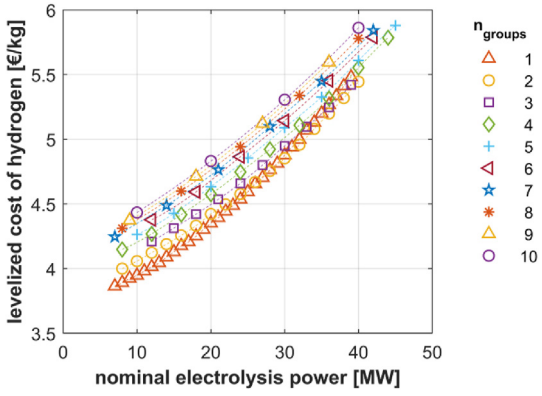

Fig. 10 – Levelized cost of hydrogen (LCOH) *vs* overall nominal electrolysis power for a different number of electrolysis groups.

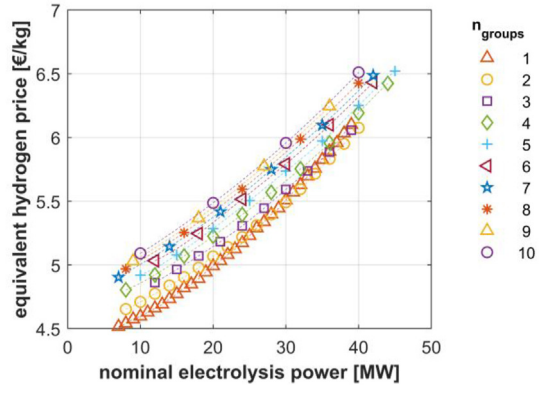

Fig. 11 – Equivalent hydrogen price (EHP) *vs* overall nominal electrolysis power for a different number of electrolysis groups.

grid. At the same electrolysis capacity, the EHP of the configuration with only one group is the lowest for nominal capacities of up to about 28 MW. At higher electrolysis capacities, the lowest EHP is found with two groups because the higher hydrogen production overcomes the higher specific BoP cost in comparison to the configuration with only one group.

By fixing several hydrogen selling prices, the annual gain difference (Eq. (28)) with respect to the case in which there is not an electrolysis system, and all the wind electricity is sold to the grid has been evaluated (Fig. 12, graphs on the left). It shows a maximum for a certain value of the overall electrolysis capacity which depends on the hydrogen price. Indeed, at low overall electrolysis capacities, an increase in the overall capacity produces an increase in hydrogen production that is sufficient to overcome the increase in the capital costs. Instead, at high overall capacities, the increase in the capital

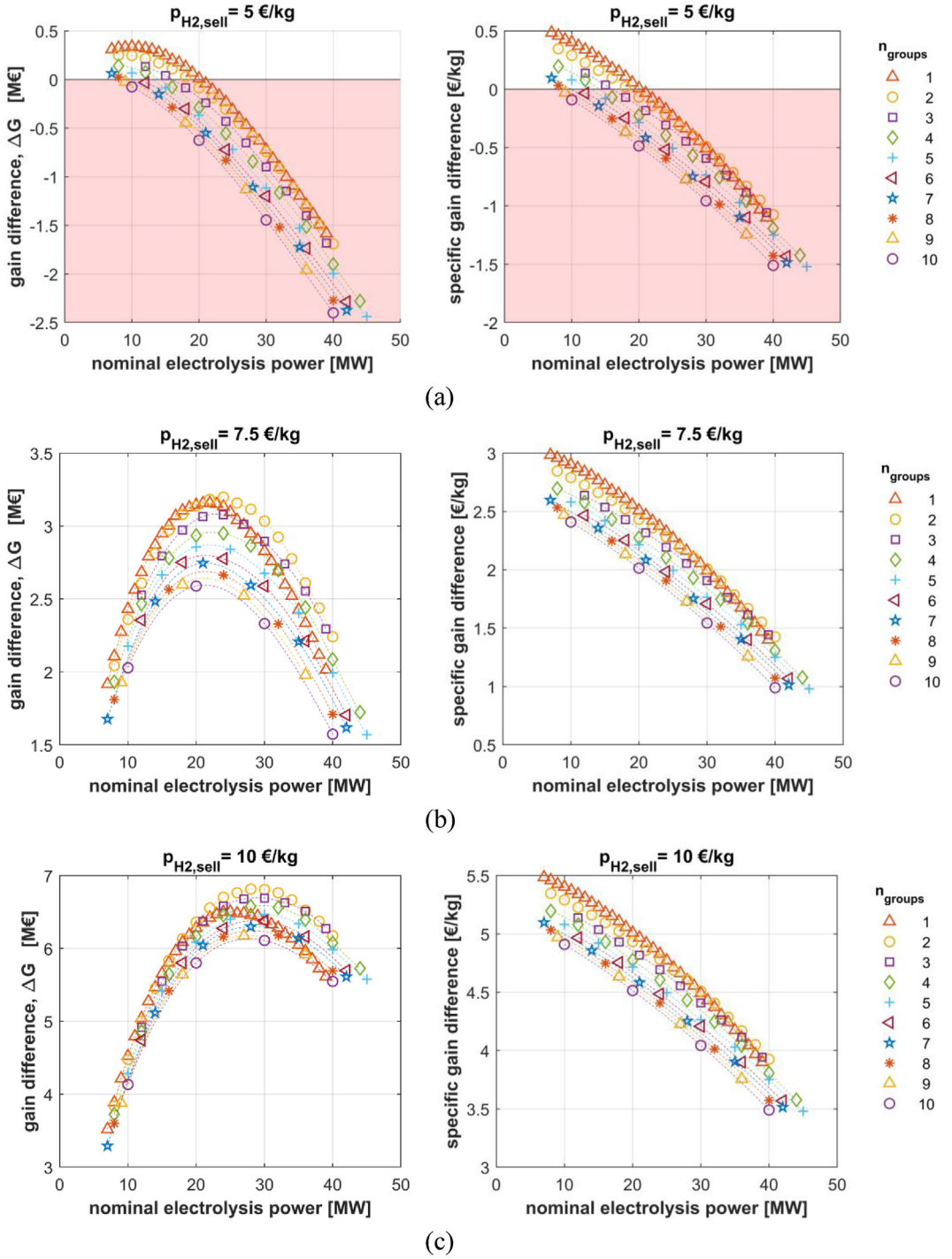

Fig. 12 – Annual gain difference (graphs on the left) and corresponding annual specific gain difference (graphs on the right) *vs* overall nominal electrolysis power for a different number of electrolysis groups with a hydrogen selling price ($p_{H_2,sell}$) of (a) 5 €/kg, (b) 7.5 €/kg, and (c) 10 €/kg.

costs is not compensate by an adequate income from the increased hydrogen production. The electrolysis plant capacity giving the maximum gain difference increases for increasing hydrogen selling prices because of the increased specific income from selling hydrogen.

At lower overall electrolysis capacities, at the same capacity, the gain difference is the highest for the configuration with only one group. At a hydrogen selling price of 7.5 €/kg or higher, the maximum gain difference is obtained with two groups and at an overall capacity that increases with the hydrogen selling price. The maximum gain is obtained with a single group with a nominal capacity of 10 MW when $p_{H_2,sell} = 5$ €/kg, with two groups and an overall nominal electrolysis capacity of 24 MW when $p_{H_2,sell} = 7.5$ €/kg, and with two groups and an overall nominal electrolysis capacity of 28 MW when $p_{H_2,sell} = 10$ €/kg.

The specific gain difference per kilogram of hydrogen decreases with the overall electrolysis capacity (Fig. 12, graphs on the right), coherently with the opposite trend of EHP. At the same overall electrolysis capacity, the highest specific gain differences are obtained with one group up to a nominal electrolysis power of 28 MW. By further increasing the overall electrolysis capacity, slightly higher maximum specific gain differences are obtained with two groups.

Conclusions

Several configurations of an alkaline electrolysis system for green hydrogen production from a 39 MW-wind farm were compared by analyzing techno-economic indicators. The effect of both the size of the electrolysis plant and the number of separated groups into which it is divided was investigated. Three operational states were considered for each group: on, stand-by, and off states. The model adopted took into account stack degradation as a function of the equivalent operating hours and the number of start-ups from the off state.

The main findings are:

- Most of the OFF periods have a duration of less than 6 h. This result suggests investigating the possibility of both adding electrical storage or allowing grid support during short periods of low wind power in order to reduce the number of OFF periods. The effect on CO_2 emissions per kilogram of produced hydrogen should be evaluated since a small increase in specific emissions could allow to obtain both a more continuous production and a significant reduction in specific costs by increasing the electrolyzer utilization factor and reducing stack degradation.
- When the overall nominal electrolysis power is greater than half the wind one, higher hydrogen production is obtained with configurations with two groups instead of those with only an equivalent bigger group. The difference becomes more marked for increasing overall electrolysis capacities. A further increase in the number of groups does not influence much hydrogen production.
- The lower is the electrolysis capacity, the lower is LCOH. At the same electrolysis capacity, the lowest LCOH is obtained in the configurations with only one group for a nominal electrolysis power of up to about 28 MW. At higher electrolysis capacities, the lowest LCOH is obtained with two groups.
- The equivalent hydrogen price (EHP), defined as the selling price at which the net income obtained is the same as that in the case without an electrolysis plant in which all the wind electricity is sold to the grid, increases with the overall electrolysis capacity, and varies between 4.5 and 6.5 €/kg, depending on the configuration. Configurations with only one or two groups, depending on the hydrogen selling price, give the maximum net income at an overall nominal power increasing with the hydrogen selling price and resulted the most profitable.

Declaration of competing interest

The authors declare that they have no known competing financial interests or personal relationships that could have appeared to influence the work reported in this paper.

Nomenclature

Symbols

C	cost [€]
c	specific cost [€/MWh]
C_{cw}	cooling water thermal capacitance [J/K]
C_{th}	electrolyzer thermal capacitance [J/K]
E	annual energy [MWh]
$h_{eq\ max}$	maximum equivalent operating hours before stack replacement is needed [h]
$h_{eq,degr}$	equivalent operating hours for degradation [h]
F	Faraday constant ($F = 96485$ C/mol)
ΔG	annual gain difference [€]
I	current [A]
i	current density [A/m^2]
k	index for the time step
L_{degr}	degradation level
Lt	lifetime [y]
$M_{H_2,ann}$	annual hydrogen production [kg]
$\dot{n}_{H_2}$	hydrogen production rate [mol/s]
n_{cells}	number of stack cells
n_{groups}	number of electrolysis groups
$n_{elz\ per\ group}$	number of electrolyzers in each group
$n_{OFF\rightarrow ON}$	number of state transitions from OFF to ON
n_{repl}	number of stack replacements
P	power [W]
Q	heat [W]
p	price [€/MWh]
$p_{H_2\ sell}$	hydrogen selling price [€/kg]
R_{th}	overall electrolyzer thermal resistance [K/W]
T	temperature [°C]
U	voltage [V]
UA_{hx}	product of the global heat transfer coefficient and the heat transfer area of the exchanger [W/K]
Δt	time step [s]
η_F	Faraday efficiency

Subscripts/superscripts

a	ambient

ann	annual, annualized
cap	capital
cw	cooling water
cwi	cooling water inlet
cwo	cooling water outlet
cool	cooling
degr	degradation
el	electrical energy
elz	electrolyzer
gen	generated
nom	nominal
purch	purchase
O&M	operation and maintenance
pl	plant
repl	replacement
rev	reversible
SB el	grid electricity for SBs
sell	selling
tn	thermo-neutral
w	wind
w el	wind electricity
grid→elz sys (SB)	from the grid to the electrolysis system for SBs
w→elz sys	from the wind farm to the electrolysis system
w→grid	from the wind farm to the grid

Acronyms

BoP	balance of plant
CRF	capital recovery factor
EHP	equivalent hydrogen price [€/kg H_2]
IR	interest rate
LHV	lower heating value
LCOH	levelized cost of hydrogen
PV	photovoltaic
RE	renewable energy

REFERENCES

[1] IEA. The Future of Hydrogen: seizing today's opportunities. 2019. Available online: https://www.iea.org/reports/the-future-of-hydrogen.

[2] Liponi A, Pasini G, Baccioli A, Ferrari L. Hydrogen from renewables: is it always green? The Italian scenario. Energy Convers Manag 2023;276:116525. https://doi.org/10.1016/j.enconman.2022.116525.

[3] Egeland-Eriksen T, Hajizadeh A, Sartori S. Hydrogen-based systems for integration of renewable energy in power systems: achievements and perspectives. Int J Hydrogen Energy 2021;46:31963–83. https://doi.org/10.1016/j.ijhydene.2021.06.218.

[4] Dolci F. Green hydrogen opportunities in selected industrial processes: workshop summary report (26th of June 2018, Centre Albert Borschette, Brussels, Belgium). Luxembourg: Publications Office of the European Union; 2018. 978-92-79-99135-6.

[5] Schmidt O, Gambhir A, Staffell I, Hawkes A, Nelson J, Few S. Future cost and performance of water electrolysis: an expert elicitation study. Int J Hydrogen Energy 2017;42:30470–92. https://doi.org/10.1016/j.ijhydene.2017.10.045.

[6] Hernández-Gómez Á, Ramirez V, Guilbert D. Investigation of PEM electrolyzer modeling: electrical domain, efficiency, and specific energy consumption. Int J Hydrogen Energy 2020;45:14625–39. https://doi.org/10.1016/j.ijhydene.2020.03.195.

[7] Götz M, Lefebvre J, Mörs F, McDaniel Koch A, Graf F, Bajohr S, Reimert R, Kolb T. Renewable Power-to-Gas: a technological and economic review. Renew Energy 2016;85:1371–90. https://doi.org/10.1016/j.renene.2015.07.066.

[8] Brauns J, Turek T. Alkaline water electrolysis powered by renewable energy: a review. Processes 2020;8:248. https://doi.org/10.3390/pr8020248.

[9] Abdel Haleem A, Huyan J, Nagasawa K, Kuroda Y, Nishiki Y, Kato A, Nakai T, Araki T, Mitsushima S. Effects of operation and shutdown parameters and electrode materials on the reverse current phenomenon in alkaline water analyzers. J Power Sources 2022;535:231454. https://doi.org/10.1016/j.jpowsour.2022.231454.

[10] Ali Khan MH, Daiyan R, Han Z, Hablutzel M, Haque N, Amal R, MacGill I. Designing optimal integrated electricity supply configurations for renewable hydrogen generation in Australia. iScience 2021;24:102539. https://doi.org/10.1016/j.isci.2021.102539.

[11] Liponi A, Frate GF, Baccioli A, Ferrari L, Desideri U. Impact of wind speed distribution and management strategy on hydrogen production from wind energy. Energy 2022;256:124636. https://doi.org/10.1016/j.energy.2022.124636.

[12] Abbas MK, Hassan Q, Tabar VS, Tohidi S, Jaszczur M, Abdulrahman IS, Salman HM. Techno-economic analysis for clean hydrogen production using solar energy under varied climate conditions. Int J Hydrogen Energy 2023;48:2929–48. https://doi.org/10.1016/j.ijhydene.2022.10.073.

[13] Liponi A, Frate GF, Baccioli A, Ferrari L, Desideri U. Green hydrogen from wind energy: mitigation of operating point fluctuations. In: Proceedings of ECOS - the 34th international conference on efficiency, cost, optimization, simulation and environmental impact of energy systems; 2021. Taormina, Italy, June 27-July 2.

[14] Fang R, Liang Y. Control strategy of electrolyzer in a wind-hydrogen system considering the constraints of switching times. Int J Hydrogen Energy 2019;44:25104–11. https://doi.org/10.1016/j.ijhydene.2019.03.033.

[15] Matute G, Yusta JM, Beyza J, Correas LC. Multi-state techno-economic model for optimal dispatch of grid connected hydrogen electrolysis systems operating under dynamic conditions. Int J Hydrogen Energy 2021;46:1449–60. https://doi.org/10.1016/j.ijhydene.2020.10.019.

[16] Zheng Y, You S, Bindner HW, Münster M. Optimal day-ahead dispatch of an alkaline electrolyser system concerning thermal–electric properties and state-transitional dynamics. Appl Energy 2022;307:118091. https://doi.org/10.1016/j.apenergy.2021.118091.

[17] Varela C, Mostafa M, Zondervan E. Modeling alkaline water electrolysis for power-to-x applications: a scheduling approach. Int J Hydrogen Energy 2021;46:9303–13. https://doi.org/10.1016/j.ijhydene.2020.12.111.

[18] Lu X, Du B, Zhou S, Zhu W, Li Y, Yang Y, Xie C, Zhao B, Zhang L, Song J, et al. Optimization of power allocation for wind-hydrogen system multi-stack PEM water electrolyzer considering degradation conditions. Int J Hydrogen Energy 2022;48:5850–72. https://doi.org/10.1016/j.ijhydene.2022.11.092.

[19] Hong Z, Wei Z, Han X. Optimization scheduling control strategy of wind-hydrogen system considering hydrogen production efficiency. J Energy Storage 2022;47:103609. https://doi.org/10.1016/j.est.2021.103609.

[20] Luxa A, Jöres N, Yáñez C, Souza M, Pangalos G, Schnelle L, Lichtenberg G. Multilinear modeling and simulation of a multi-stack PEM electrolyzer with degradation for control

concept comparison. 14/07/2022 - 16/07/2022. In: Proceedings of the 12th international Conference on Simulation and modeling methodologies, Technologies and applications. Lisbon, Portugal: SCITEPRESS - Science and Technology Publications; 2022. p. 52–62. 978-989-758-578-4.
[21] Rizwan M, Alstad V, Jäschke J. Design considerations for industrial water electrolyzer plants. Int J Hydrogen Energy 2021;46:37120–36. https://doi.org/10.1016/j.ijhydene.2021.09.018.
[22] MATLAB and statistics toolbox release. The MathWorks, Inc; 2019a.
[23] Power technology website. Available online: https://www.power-technology.com/marketdata/lake-bonney-australia/.
[24] Sakas G, Ibáñez-Rioja A, Ruuskanen V, Kosonen A, Ahola J, Bergmann O. Dynamic energy and mass balance model for an industrial alkaline water electrolyzer plant process. Int J Hydrogen Energy 2022;47:4328–45. https://doi.org/10.1016/j.ijhydene.2021.11.126.
[25] Ulleberg O. Modeling of advanced alkaline electrolyzers: a system simulation approach. Int J Hydrogen Energy 2003;28:21–33. https://doi.org/10.1016/S0360-3199(02)00033-2.
[26] Armijo J, Philibert C. Flexible production of green hydrogen and ammonia from variable solar and wind energy: case study of Chile and Argentina. Int J Hydrogen Energy 2020;45:1541–58. https://doi.org/10.1016/j.ijhydene.2019.11.028.
[27] Schnuelle C, Wassermann T, Fuhrlaender D, Zondervan E. Dynamic hydrogen production from PV & wind direct electricity supply – modeling and techno-economic assessment. Int J Hydrogen Energy 2020;45:29938–52. https://doi.org/10.1016/j.ijhydene.2020.08.044.
[28] Böhm H, Zauner A, Rosenfeld DC, Tichler R. Projecting cost development for future large-scale power-to-gas implementations by scaling effects. Appl Energy 2020;264:114780. https://doi.org/10.1016/j.apenergy.2020.114780.
[29] Olateju B, Kumar A, Secanell M. A techno-economic assessment of large scale wind-hydrogen production with energy storage in Western Canada. Int J Hydrogen Energy 2016;41:8755–76. https://doi.org/10.1016/j.ijhydene.2016.03.177.
[30] IRENA. Renewable power generation costs in 2019. 2020. Abu Dhabi.